UNIVERSITÀ DEGLI STUDI DI PADOVA

Dipartimento di Fisica e Astronomia "Galileo Galilei"

Corso di Laurea in Fisica

Tesi di Laurea

Development and Validation of ML-based trigger algorithms

Relatore

Prof. Marco Zanetti

Correlatore

Prof. Jacopo Pazzini

Laureando

Giacomo Franceschetto

Anno Accademico 2020/2021

Abstract

Complex machine learning (ML) based algorithms are finding their ways to low-level hardware devices like FPGAs. A neural network model is being implemented for the online identification and trigger of the passage of charged particles through a drift-tubes detector and for the reconstruction of its trajectory; such model is being tested on a set of such detectors operating at Legnaro INFN National Laboratory (LNL) with cosmic muons. The ultimate goal is to deploy this algorithm on the trigger system of the muon spectrometer of CMS at the LHC.
The thesis work describes the performances of such algorithms, studying the data collected in Legnaro, and further develop it to extend its acceptance.

Contents

Introduction

Muons play a crucial role in the principal experiments conducted at CERN LHC, especially at the Compact Muon Solenoid (CMS). From the fact that they are the only detectable particles to go across the whole detector without significant loss of energy, muons are widely used for the identification of interesting events among the large number of collisions provided by LHC. Hence, the detection and reconstruction of the passage of muons with high efficiency is a key feature in these experiments. The CMS trigger system [4] receives data at an event rate of 40MHz and reduces it to approximately 1kHz in two stages: the first (Level 1) consists of algorithms implemented on custom electronics based on Field Programmable Gate Arrays (FPGAs), the second based on software reconstruction run on a computing farm. These algorithms and techniques have to cope with demanding conditions such as background noise and the short time available for trigger decision, currently of the order of $3\,\mu s$ for the Level 1 trigger, and as a result, they are often modified and optimized during data taking.

A novel approach [6] consists in the implementation of an algorithm mixing artificial neural networks and analytical methods on a FPGA for muons identification and track parameter estimation, the outputs of these analyses are referred to as *online reconstruction*. This algorithm is being tested on a cosmic muon telescope at the Legnaro INFN National Laboratory (LNL), a detector composed by a set of drift-tubes (DT) reproducing a small-scale replica of those in use at CMS. Dimensions of DTs, base geometry of their arrangement, and event rate acquisition are the same as CMS's muons chambers.

In this thesis, a data-analysis framework is developed to perform a parallel offline analysis on the data collected at LNL, from which the positions of the muons in the DTs can be reconstructed and the parameters of his track estimated. Thanks to this information, it is possible to analyze the performance of the online reconstruction. The experimental setup at LNL is outlined in Chapter 1; Chapters 2 and 3 provide a description of the data formats and how they are analyzed in the offline reconstruction; the following one discusses the performance of the online reconstruction and presents the principal results obtained; the final chapter explores the challenges in extending the online reconstruction at large scales.

Chapter 1

Experimental setup

1.1 Drift tube detector

1.1.1 Drift tube cell

The elementary units of the detector are cells with a cross section of L x $h = 42$ x $13\,mm^2$ filled with an Ar-CO_2 (85/15%) gas mixture kept at atmospheric pressure. Each cell contains an anodic wire at high voltage potential, $V_{\text{wire}} = +3600V$, while the side walls cathodes are at $V_{\text{cathode}} = -1800V$. In order to provide a uniform electric field two additional electrodes are mounted on the top- and bottom-wall, kept at $V_{\text{strip}} = -1200V$. At the passage of an ionizing particle, electrons are knocked off the gas atoms, then they follow the electric field ending up at the positively charged wire, moving at an almost constant drift velocity of $v_d \approx 54\,\mu m/ns$. The charge deposited on the wire produces an electrical signal that can be used for measuring the arrival time of the electronic cloud. This collected time t contains information about the muon arrival time and the drift time t_d. Drift time is the time taken by the ionization to reach the wire thanks to the constant drift velocity due to the specific electrodes configuration, and it is proportional to the distance between the passage position of the muon and the wire x. It is possible to compute t_d subtracting from t the contribution of an unknown time pedestal t_0. This time pedestal is a parameter that contains contributions due to the trigger time and due to the time necessary for the electronics to detect and collect data.

$$x = v_d t_d = v_d(t - t_0) \tag{1.1}$$

1.1.2 Super-layer

A layer is a set of 16 cells, one beside the other. A super layer (SL) is composed by 4 stacked layers, for a total of 64 cells. In a SL, the layers are staggered by half a cell, as shown in Figure 1.1.

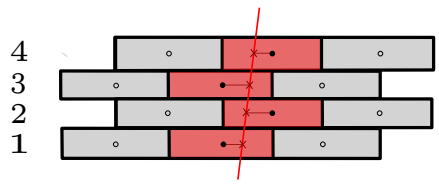

Figure 1.1: Staggered configuration of layers

One of the main features of these SLs is their trigger capability. Thanks to the geometrical configuration of the layers, a set of equations based on the mean timer technique [2] can be exploited to relate the passage time of the track in multiple cells and to compute the time pedestal. Therefore, a trigger can be directly generated from the hits data. For the particular case of Figure 1.1, the following relation holds:

$$T_{\text{MAX}} = t_{d_2} + \frac{t_{d_1} + t_{d_3}}{2} \tag{1.2}$$

where $t_{d_i} = t_i - t_0$ are the drift times of three consecutive layers (numbered from bottom to top) and T_{MAX} represents the maximum drift time allowed by the cell dimensions, $T_{\text{MAX}} = \frac{L/2}{v_d} \approx 390\,ns$.

1.2 Muon telescope setup

The setup with which the majority of the data analyzed were taken is composed by 4 SLs, 3 with the same view (θ) and one rotated by $\pi/2$ around the z-axis (ϕ view). This rotated SL is meant to provide a 3D track reconstruction that will not be covered in this work, therefore all analyses will be referred to the XZ projection shown in Figure 1.2 (b).

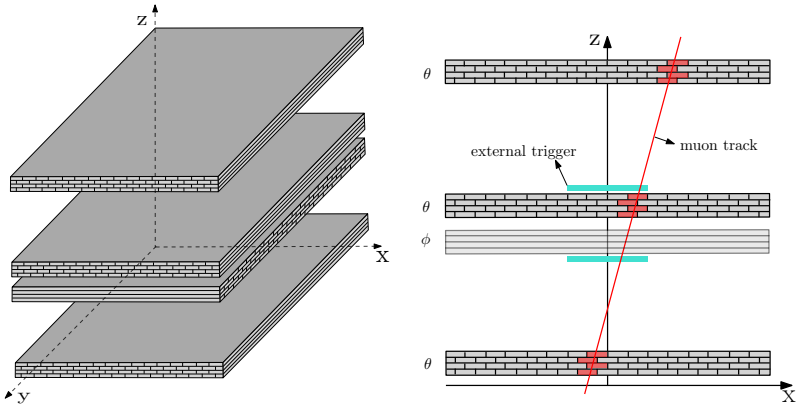

(a) *3D view* (b) *2D view - XZ projection*

Figure 1.2: LNL experimental setup

The two external SLs are arranged at approximately 80 cm from the middle ones. A pair of scintillators, placed around the central SLs of the telescope, are read out in coincidence providing an external trigger. The timing references of muons tracks, from which we can perform the offline analysis, can be obtained from the scintillator's coincidence.

1.2.1 Setup configurations studies

Further analyses performed in the context of this thesis have shown that, at these distances between the SLs, the multiple scattering of muons through the detector's components cannot be ignored. It worsens noticeably the position resolution that can be achieved by combining the measurement of all SLs in a global reconstruction with respect to the local one performed online. As a result, a change of the setup configuration has been proposed to minimize the impact of the multiple scattering on the trigger performance estimation. Currently, the SLs are arranged at shorter distances, at about 16 cm.

Other studies have been made considering the impact of the addition of a layer of lead before the second scintillator with the aim of stopping the softest muons that are more affected by multiple scattering. Having available only 9 cm of material, and due to the geometrical constraints of the setup, the additional layer was suitable for shielding only a small region of the cosmic muons spectrum. The average energy loss through the lead layer was about $\approx 115\,MeV$ and the average energy of a cosmic muon is $\mathcal{O}(1\,GeV)$. Consequently, this complementary solution was not implemented.

Chapter 2

Preprocessing and Data format

2.1 Data format

Every time a wire within a cell receives a signal greater than a predefined threshold, the detectors' data acquisition system injects the digitized time (TDC) hit information into the data stream. Every record is codified in a data format containing 6 fields [1]:

- *HEAD* is an ancillary information used to discriminate among different kinds of data
- $FPGA \in [0, 1]$ and $TDC\_CHANNEL \in [0, 127]$ are integers providing the location of the cell in the detector, i.e. the layer and SL of belonging
- *ORB_CNT*, *BX* and *TDC_MEAS* are also integers from which the timing information in ns can be calculated: $t = ORB\_CNT{}^{*}3564{}^{*}25 + BX{}^{*}25 + TDC\_MEAS\ {}^{*}25/30$

Other special rows are appended to the hit records for storing additional information from both internal and external triggers, including the track reconstruction parameters of the muons in a limited section of the detector where the internal trigger algorithm is implemented.

2.2 Event selection

The collection of all the hits produced by the muon traversing the detector is referred to as *event*. As one orbit corresponds to roughly $90\mu s$, the probability of getting two muons within the same orbit is very small. It has been assumed that all the hits in the same orbit (*ORBT_CNT* parameter) of an external trigger hit can be gathered in an event.

Selecting events with this procedure, it is plausible that among the "physical" hits due to the passage of the muon there will be some "noise" hits, either due to electronic-induced noise or from other particles, such as delta rays, producing ionization. Both online and offline reconstruction have to deal with the task of detecting genuine muons hits. Having a 12 layer detector (in the 2D projection considered), we expect events of 12 hits plus noise. In some cases, we observe events composed by a number of hits considerably greater compared to expectations. These occurrences will be excluded from the analysis and correspond to cosmic rays "showers".

2.3 Time calibration and mapping

In this section, the focus is pointed on calculating the position of the hit within the cell. As has been shown in Equation 1.1, this task can be done using the information of the drift time. However, having only t and not t_d, a calibration of the the timing information received from the DT cells is necessary.

Starting from the event selection, the external trigger time (t_{SCINT}) linked to every group of hits can be used. To obtain the drift time, it can be considered that:

$$t_d = t - t_0 = t - t_{\text{SCINT}} - \text{SCINT\_offset} - \text{SL\_offset} \tag{2.1}$$

where *SCINT_offset* is a delay due to electronics and cables of the external trigger and *SL_offset* is due to the detector geometry, muons traverse different SLs in different times. The drift times distributions are expected to be almost uniform from 0 to $\approx 390\,ns$, the maximum drift time, so they are referred to as time boxes. Therefore, it is possible to obtain the offsets by drawing the time box of $t - t_{\text{SCINT}}$, where t_{SCINT} differs event by event, and applying a time shift such that the new time box has the rising edge at the starting time of $0\,ns$. An example of time calibration is shown in Figure 2.1 (a).

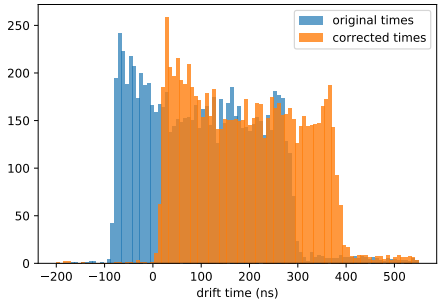

Figure 2.1: Time boxes before (blue) and after (orange) the application of the calibration procedure

Next, the distance of the hit from the wire can be simply estimated using drift time and velocity. The task of computing the global x position of the hit is performed by the offline reconstruction algorithm because, at this point, there is still the left-right ambiguity: the exact distance between the hit and the wire is known but it is unclear if the particle track is to the left or to the right of the wire.

2.4 Indirect measurement of electron drift velocity

At this stage, a measurement of the drift velocity can be computed combining drift times in one of the mean timer equations. Care must be taken in selecting only the events that follow the pattern of the equation used. Specifically, only events like the one shown in Figure 1.1 have been considered, labeling them as *123* or *234* depending on which layers the current event covers. For both patterns, the Equation 1.2 can be used.

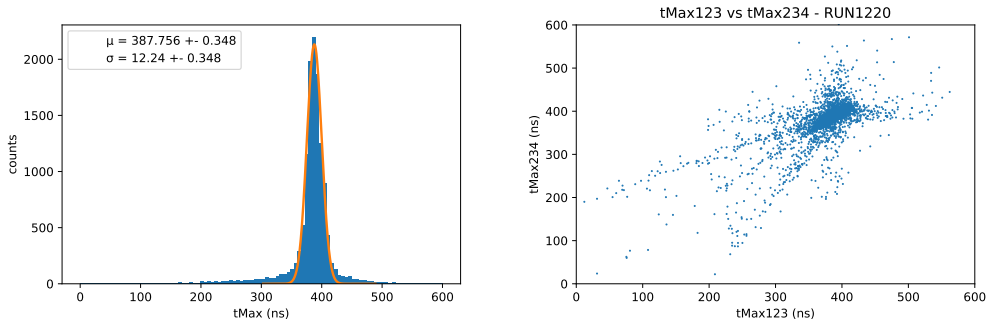

(a) *TMax* (b) *TMax 123 vs 234*

Figure 2.2: TMax measured in 123 and 234 patterns

In Figure 2.2 (a) it has been represented the total distribution of the TMaxs calculated. In (b),

instead, for those events where both patterns can be considered, a scatter plot of TMaxs computed in *123* vs *234* is reported. The former picture provides a value for TMax as the mean of the Gaussian fit and allows to estimate the drift velocity as $v_d = \frac{L/2}{TMax} = 54.16 \pm 0.05\,\mu m/ns$ [2]. The obtained v_d is consistent with the one expected [3] .
In the latter picture, 4 major features can be easily distinguished:

(i) 2 distribution of measures for which one TMax is correctly around $390\,ns$ and the other is not

(ii) 2 distribution of measures for which both TMax are far from the expectation

Distribution (i) corresponds to the physical case of delta-ray emission in one of the external layers while (ii) reflects a delta-ray in the central layer. Delta-rays are due to electrons knocked out of gas atoms that have enough energy to ionize again and, when emitted, they can obscure the original signal.

Chapter 3

Offline track reconstruction algorithm

3.1 Local reconstruction

Given a set of hits forming an event, separate subsets are created and each one is filled with hits belonging to a single SL.

3.1.1 Hits grouping

In each subset, the minimal condition for the mean timer equation viewed in Equation 1.2, and therefore also for the online reconstruction with which we want to compare results, is to have at least 3 signals in 3 different layers. Consequently, subsets where there are less than 3 hits are excluded from the analysis. Next, all the possible combinations of 4 hits in 4 different layers (or only one combination of 3 hits if we have the minimal condition seen before) within a single SL are stored. As a result, all permitted patterns for the muon track are considered. However, the left-right ambiguity in the x global position of the hit is still present. To solve this, the left-right possibilities are merged in a single list and combined in groups of 4, taking care of gathering only elements with different z coordinates.

3.1.2 Track parameters estimation

The estimation of the track parameters is simply made iterating over the second stage combinations obtained before and performing a linear regression. The interpolation considers the z coordinate as abscissa of negligible error and the x as ordinate with standard deviation of $400\,\mu m$, derived from previous analyses:

$$x = m \cdot z + q \tag{3.1}$$

Best fit values are selected among the various groups of hits minimizing the χ^2 compatibility, computed as:

$$\lambda_{\chi^2} = \frac{|\chi^2 - d.o.f.|}{\sqrt{2 d.o.f.}}, \quad d.o.f. = N - 2 \tag{3.2}$$

where N is the number of hits considered (4 or 3).

3.2 Global reconstruction

For the purpose of this work, a global track is defined only if the minimum number of hits to perform a local reconstruction in each SL is reached. Therefore, global events are expected to be composed by 9-12 hits. Global track parameters are estimated starting from the (z, x) points obtained from the previous local reconstructions. Since signal-noise and left-right ambiguity have already been solved, a linear regression can be directly performed bypassing the combinatorial step.

An example event-display showing global and local reconstructions is pictured in Figure 3.1, where the left-right ambiguity within a cell can also be observed (the two possibilities are marked with different colors).

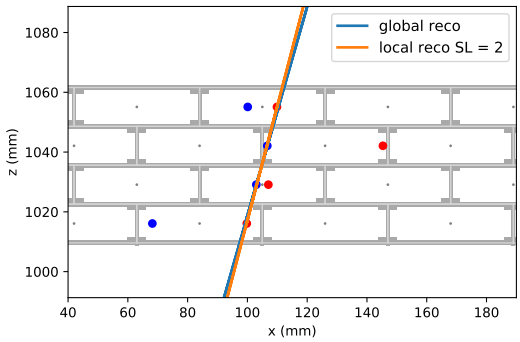

Figure 3.1: Event display zoom on SL 2

3.3 Summary plots

In this section, the results of the offline reconstruction over a standard data run are presented.
As shown in Figure 3.2 (a), angles of the local tracks with respect to the z axis vary within the range $[-25°, 25°]$. This limited interval is a consequence of the acceptance of the scintillators. In the global reconstruction case the distribution is similar. Whereas, in (b) the difference in x residuals $(x_{\text{hit}} - x_{\text{reco}})$ distributions between local and global reconstructions can be observed. Local residual resolution is, as expected, greater than the global one and both values are consistent with the 400 μm standard deviation considered in the x coordinate.

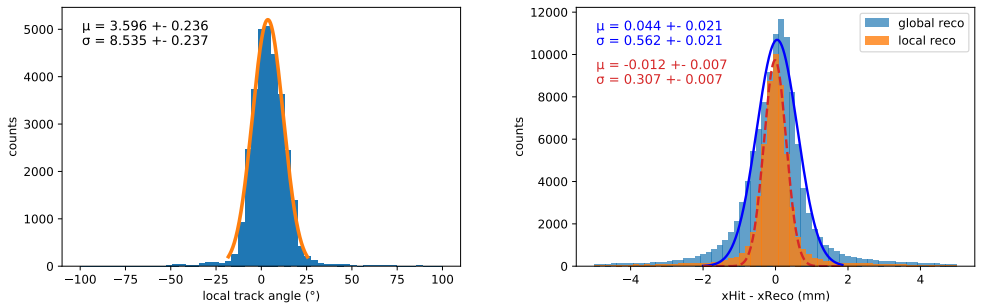

(a) *Angles distribution - local reconstruction* (b) *Local and global residuals distributions*

Figure 3.2: Offline reconstruction performances

Chapter 4

Performances of ML-based algorithm for online reconstruction

In this chapter, a comparison between offline and online reconstructions in different conditions is presented to observe and test the performances of the ML-based reconstruction algorithm.

4.1 Macrocell implementation

Online reconstruction is implemented in a FPGA and considers a section of 4×4 cells, referred here as a macrocell (MC), in the central SL with θ view (SL2). With respect to the first cell in the SL the MC is shifted by three cells ($x_{\text{shift}} = +126\,mm$) to find itself roughly in proximity of the scintillators. This module is able to provide not only an internal trigger but also angle and position information about the local track inside the specific SL.

4.2 Data run descriptions

Data runs used to analyze the performances of the online reconstruction were collected in different conditions:

- **RUN1220**: standard conditions
- **RUN1221**: 1 external layer of SL2 disconnected
- **RUN1222**: 1 internal layer of SL2 disconnected
- **RUN1223**: lower threshold for detecting signal, i.e. more noise is expected within collected data

4.3 Efficiency

The z coordinate at the center of SL2 has been defined as $\overline{z}$ and the x coordinate at half of the MC as $\overline{x}$. Given that a MC is composed by 4 cell for each layer and L is the x length of a cell, efficiency of online reconstruction is computed as: [1]

$$\text{eff} = \frac{\text{denominator AND trigger of the online reconstruction}}{\text{offline global traces where } x(\overline{z}) \in [\overline{x} - 1.5L; \overline{x} + 1.5L]} \tag{4.1}$$

	RUN1220	RUN1221	RUN1222	RUN1223
eff	0.975 ± 0.002	0.971 ± 0.003	0.974 ± 0.003	0.970 ± 0.003

[1] Uncertainties on efficiencies are computed following the bayesan approach reported in [5].

It can be noticed that the internal trigger is highly efficient, around 97%, and also that the efficiency is robust under the varying conditions.

4.4 Time resolution

A measurement of how accurate the internal trigger performed by the online reconstruction is can be done thanks to the external trigger installed on the experimental setup. In Figure 4.1, the difference $t_{\text{INT\_TRIGG}} - t_{\text{SCINT}}$ is shown for each dataset, the mean of the Gaussian interpolation of this quantity can be used as an estimate of the offset due to the scintillator electronics.

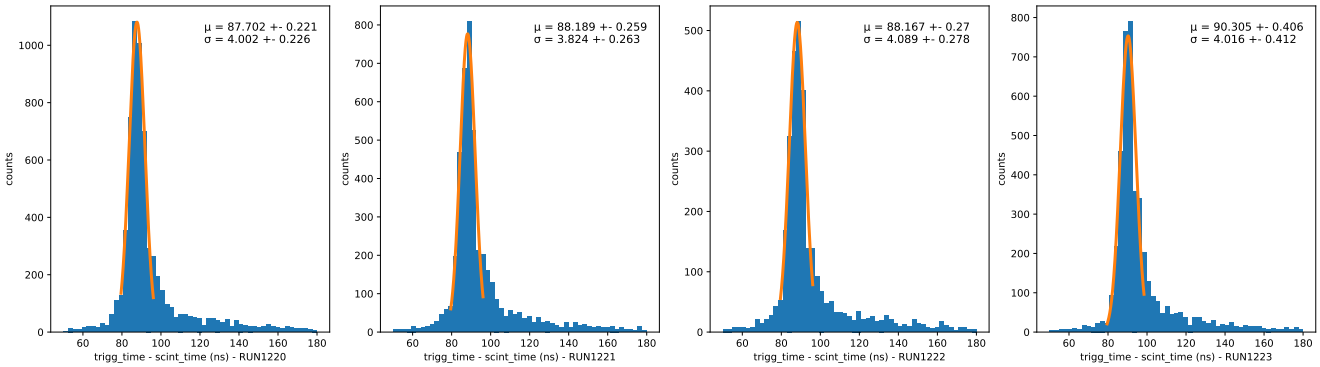

(a) (b) (c) (d)

Figure 4.1: Resolution of time difference between internal trigger and scintillator

The σ of the time difference distribution can be taken as the time resolution of the internal trigger. In the reference run its value is $4.0 \pm 0.2\, ns$ and it stays approximately constant in the other cases.

4.5 Position resolution

The position resolution is computed taking as reference the coordinate $\overline{z}$. The comparison of the local online reconstruction with the local offline reconstruction in SL2 is labeled as *local*, instead, the one between the local online reconstruction and the global offline reconstruction is labeled as *global*. While the former provides an intrinsic validation, in essence the identical information is used in both the online and offline reconstruction, the latter provides a more unbiased comparison as the offline global track is reconstructed from hits belonging also to other SLs that the online algorithm does not consider. Consequently, local resolution is expected to be better than global resolution. In Figures 4.2 and 4.3 the difference distributions between $x(\overline{z})$ deduced by online and local-global offline reconstructions are presented.

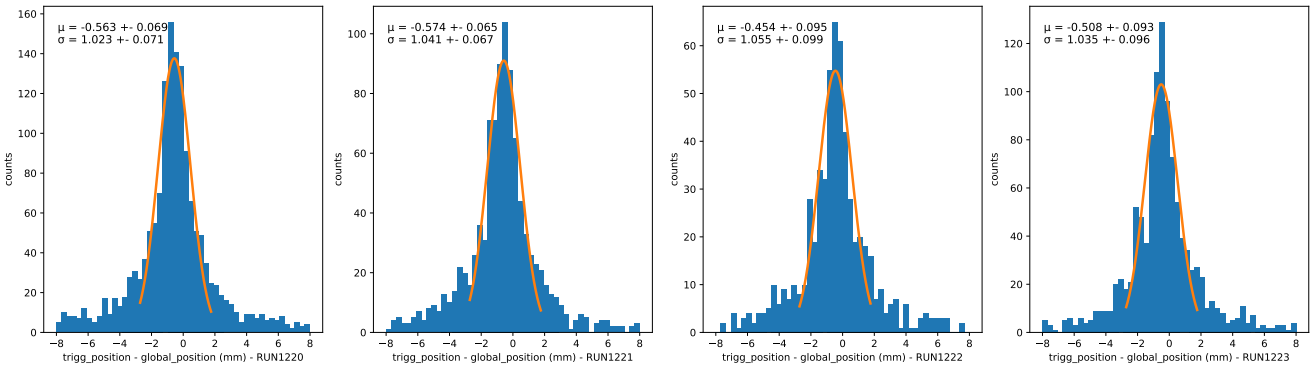

(a) *RUN1220* (b) *RUN1221* (c) *RUN1222* (d) *RUN1223*

Figure 4.2: Resolution of position difference between online and global offline reconstructions

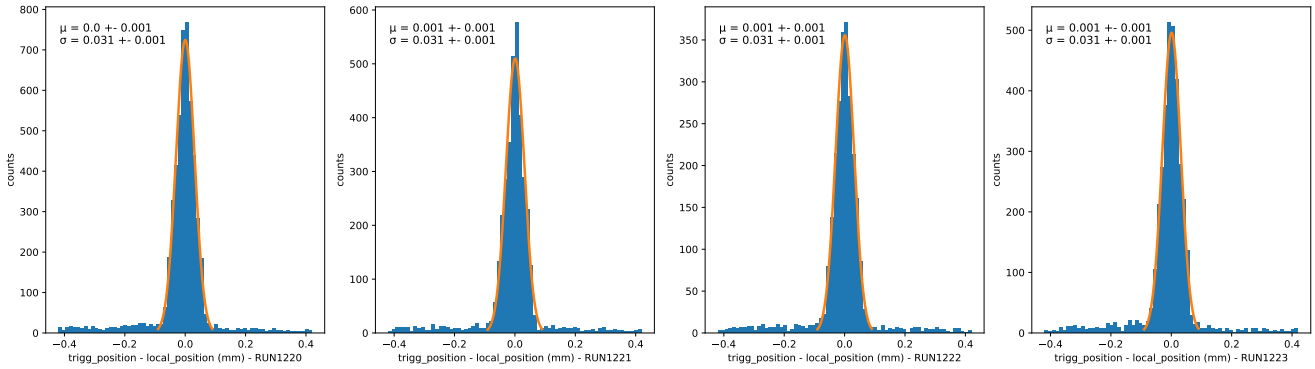

(a) *RUN1220* (b) *RUN1221* (c) *RUN1222* (d) *RUN1223*

Figure 4.3: Resolution of position difference between online and local offline reconstructions

Standard deviations of difference distributions are stable in the four datasets. However, the results display that the global resolution is about 2 orders of magnitude greater than the local one ($1.02 \pm 0.07\,mm$ versus $0.031 \pm 0.001\,mm$ for the reference run), a variation larger than expected.
This is due to the SLs arrangement of the setup that is sensible to multiple scattering. Detected muons have to go through a total of $2\,cm$ of alluminium and, therefore, for an average energy cosmic muon, the RMS of the deviation angle due to multiple scattering is expected to be $\approx 2\,mrad$. Having a total length of the detector of about $1.5\,m$, the predicted average x deviation of the trajectory is on the order of millimiters, much bigger than the resolution of x positions ($400\,\mu m$). To mitigate this effect, the previous setup has been modified by rearranging the SLs so as to lower the distance among them (less than $0.5\,m$ of total height). An analysis performed on a data run taken in this condition is shown in Figure 4.4, the increase in the global position resolution is evident.

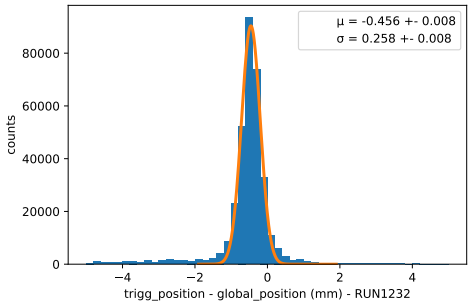

Figure 4.4: Resolution of position difference between online and global offline reconstructions with rearranged setup

4.6 Angular resolution

The angular resolution can be evaluated by comparing the online reconstruction angular parameter with either the local or the global track angle. The distribution of differences between these quantities are presented in Figures 4.5 and 4.6.

As for the position resolution, in the local case, the angular resolution is expected to be very high because both reconstructions are computed starting from the same hits. Instead, for the global case, the angular resolution is still expected to be affected by the multiple scattering, but in a smaller

amount than before. Actually, the previously estimate of the multiple scattering contribution to the global angle was $\mathcal{O}(mrad)$, so, it can be assumed that the lower resolution computed in the global reconstruction respect to the local one ($10.6 \pm 0.3\, mrad$ versus $5.8 \pm 0.3\, mrad$ for the reference run) is only due to the different hits considered. Here too, it can be noticed that there is no relevant difference in resolution between the different runs.

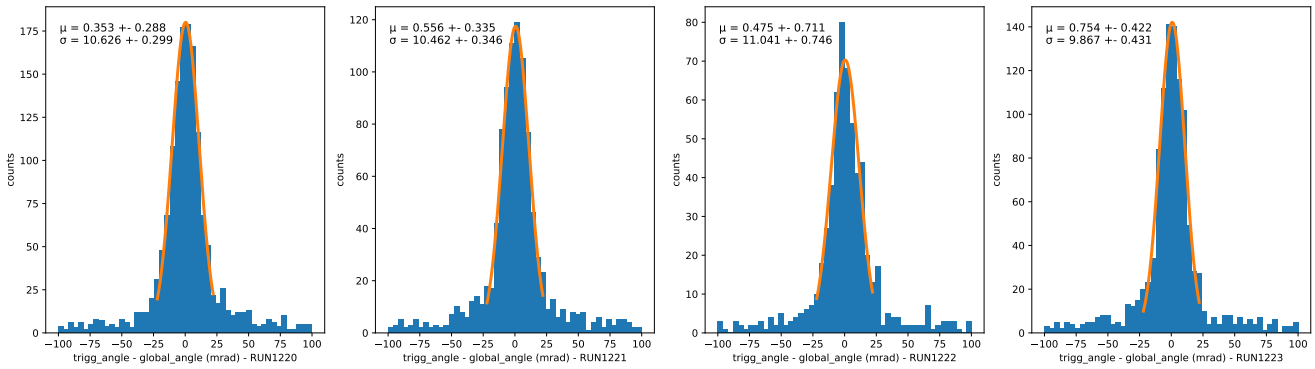

(a) (b) (c) (d)

Figure 4.5: Global angular resolution

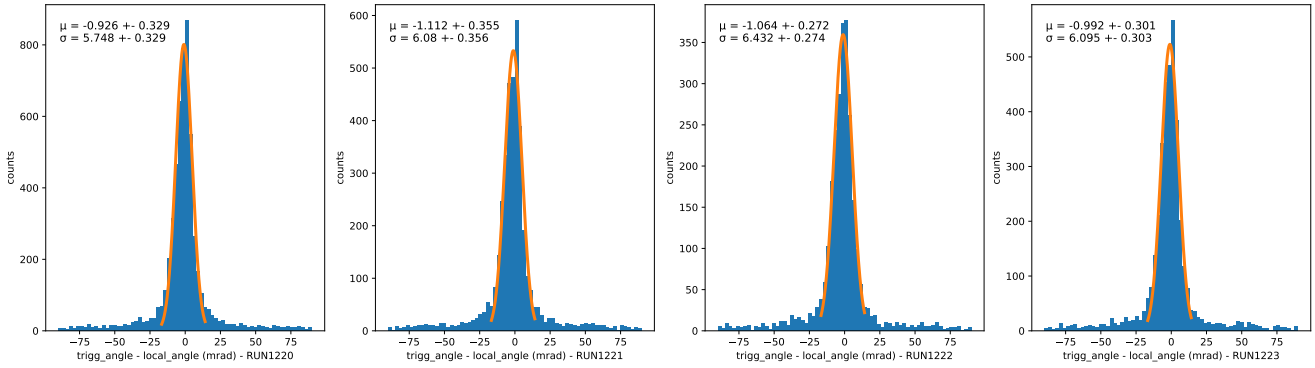

(a) (b) (c) (d)

Figure 4.6: Local angular resolution

Chapter 5

Additional studies for trigger updates

5.1 Macrocell extension

An horizontal extension of the online reconstruction algorithm, to cover not only a section of 4 cells but the whole SL, is under study. By simply replicating consecutive MCs within the chamber, there is a considerable probability that a muon passes at the ends of two adjacent entities without being triggered. To avoid this, MCs can be arranged introducing an overlap (OL = n) of $4 * n$ channels, a view of two MCs with different OL values is shown in Figure 5.1.

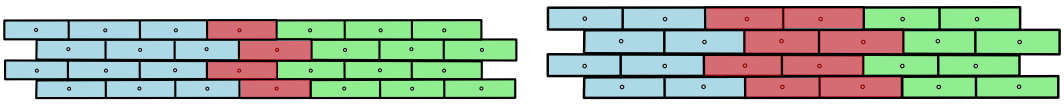

(a) (b)

Figure 5.1: MC extension with OL = 1 (a), 2 (b)

The optimal OL value can be found analyzing the efficiency and redundancy of the various configurations. Efficiency is defined as the events detected by the configuration with a certain OL value over the total events passed in the covered cells. At greater OL values, an increment in efficiency is expected, but also the detection of the same event in more than one MC is more probable. Redundancy is computed as the number of events triggered by two MCs over the total detected events. In Figure 5.2 a scatter plot of efficiency versus redundancy for OL = $0, 1, 2, 3$ is shown. For the maximum OL, the majority of cells are covered by three MCs, in this case when an event is detected by all three MCs the redundancy is double counted.

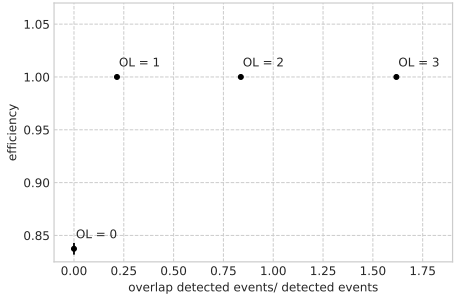

4

Figure 5.2: Efficiency vs redundancy at various OL

As can be noticed at OL = 0 there is a $\approx 15\%$ of events not detected and with just 4 cells overlapped the efficiency reaches the ideal value with a reasonably limited redundancy. These results show that

the optimal MC arrangement is expected to be with OL = 1.

The next step under development consist in a vertical extension that links local MCs belonging to different SLs, the aim of this improvement is to provide global online reconstruction of the muon traversing the detector.

Conclusions

In this thesis work, the performances of drift tubes gas detectors have been studied and a muon trigger algorithm based on neural networks has been validated.
A data-analysis framework has been developed to perform an offline track reconstruction for cosmic muons. Thanks to an external trigger, hits have been gathered in events and it was possible to compute their position within the detector. Signal-noise and left-right ambiguities were solved through a combinatorial step that allowed to obtain an estimate of muons track parameters.
The offline reconstruction results were compared with the online reconstruction provided by the internal trigger. Different conditions have been analyzed: a reference run, two runs with one layer disconnected, and a more noisy run. In all these cases the performance of the online trigger have found to be robust and no significant worsening were noticed. Overall, the algorithm has proved to be highly efficient and precise.
Lastly, an horizontal extension of the macrocell unit, where the trigger algorithm is implemented, was studied. Considering various overlap possibilities, the results confirm that with 4 cells overlapped between two consecutive macrocells an optimal efficiency with limited redundancy can be reached.

Bibliography

[1] LCP projects - Physics of Data. *Processing of triggerlessly acquired detector's data.* URL: https://github.com/PhysicsOfData/LCP_projects_Y2/blob/Group11/Project.ipynb.

[2] N. Amapane et al. *Offline Calibration Procedure of the Drift Tube Detectors.* URL: http://cds.cern.ch/record/1073687/files/NOTE2007_034.pdf?version=1.

[3] The CMS Collaboration. *Calibration of the CMS Drift Tube Chambers and Measurement of the Drift Velocity with Cosmic Rays.* URL: https://arxiv.org/pdf/0911.4895.pdf.

[4] The CMS Collaboration. *Performance of the CMS muon trigger system in proton-proton collisions at $\sqrt{s}$ = 13 TeV.* Journal of Instrumentation. URL: https://arxiv.org/pdf/2102.04790.pdf?.

[5] L. Heelan. *Calculating Efficiency Uncertainties.* URL: https://indico.cern.ch/event/66256/contributions/2071577/attachments/1017176/1447814/EfficiencyErrors.pdf.

[6] M. Migliorini et al. *Muon trigger with fast Neural Networks on FPGA, a demonstrator.* URL: https://arxiv.org/abs/2105.04428.